

## Proteomic and immunofluorescent evidence for and against the astrocyte-to-neuron lactate shuttle

Dariusz Rakus

### Abstract

Lactate got from astrocytic glycogen has been appeared to help memory arrangement in hippocampi of youthful creatures, hindering it in old creatures. Here we show, utilizing quantitative mass spectrometry-based proteomics, immunofluorescence, and qPCR that maturing is related with an expansion of glycogen digestion catalysts focus and move in their confinement from astrocytes to neurons. These progressions are went with revamping of hippocampal energy digestion which is showed by raised limit of maturing neurons to oxidize glucose in glycolysis and mitochondria, and diminished capacity for unsaturated fats use. Our perceptions recommend that astrocyte-to-neuron lactate transport may work in youthful hippocampi, in any case, during maturing neurons become free on astrocytic lactate and the metabolic crosstalk between the synapses' is disturbed.

### INTRODUCTION

During the past decade a growing body of evidence has accumulated that energy metabolism of astrocytes is a crucial player in regulation of neuronal network properties. It turned out that inhibition of glycogen breakdown and lactate release from astrocytes inhibits memory consolidation in chicks (Gibbs, Anderson, & Hertz, 2006) and disrupts memory formation and Long Term Potentiation (LTP; a molecular mechanism of memory formation) in murine hippocampi (Suzuki et al., 2011). However, all the mentioned results were obtained using young or juvenile animals (Gibbs et al., 2006; Suzuki et al., 2011).

In contrast, just recently, we have demonstrated that the inhibition of glycogen breakdown in astrocytes of old

animals significantly elevates LTP magnitude in hippocampal slices and affects the mode of dendritic spines maturation (Drulis-Fajdasz et al., 2015). In other words, inhibition of glycogen degradation in hippocampi of old animals prevents aging-associated defects in memory formation.

To obtain a deeper insight into age-associated changes we investigated the expression and localization of proteins of energy metabolism in hippocampi of young (1 month) and middle-aged (12–13 months) mice using immunofluorescent methods and a quantitative proteomics technique—total protein approach (TPA), which delivers information about the absolute (expressed in moles or moles per/mg of protein) abundance/concentration of proteins in studied samples (Wiśniewski, Hein, Cox, & Mann, 2014).

We present evidence that physiological aging process is associated with substantial changes in the expression and cellular localization of energy metabolism proteins in the hippocampal formation. Notably, glycogen metabolism enzymes expression and localization undergo significant changes which emphasizes the role of glycogen in age-related decline of cognitive functions and points to proteins involved in the regulation of glycogen metabolism in hippocampus as a targets of an anti-aging therapy.

Regardless of the controversies, our results show that the ability of aging hippocampal neurons to oxidize glucose in glycolysis becomes higher than in young ones. This is accompanied by significant elevation of mitochondrial energy metabolism and rearrangement of mitochondrial network.

The data presented here provides the most comprehensive quantitative description of energy

metabolism proteins expression in murine hippocampi during aging. It also demonstrates that, because of basically different organization of metabolism in hippocampi of young and adult/old animals, entirely different approaches to the treatment of young and aging patients suffering from medical conditions associated with energy metabolism in brain must be taken into account.

## Methods

### 2.1. Animals and tissue preparation

The experiments were performed on 2 groups of male C57BL/10J mice: young (P30,  $n = 6$ ) and aged (12 months,  $n = 6$ ). Animals were anesthetized with isoflurane and decapitated. Hippocampi were isolated in ice-cold buffer containing (in mM): NaCl 87, KCl 2.5, NaH<sub>2</sub>PO<sub>4</sub> 1.25, NaHCO<sub>3</sub> 25, CaCl<sub>2</sub> 0.5, MgSO<sub>4</sub> 7, glucose 25, sucrose 75; pH 7.4. The left hippocampi from each animal were analyzed using quantitative proteomics, the right ones were used for immunofluorescence. All the procedures were approved by the local Ethical Commission and every effort was made to minimize the number of animals used for the experiments.

### 2.2. Hippocampal lysates

Hippocampi were homogenized immediately after isolation in buffer containing 0.1 M Tris/HCL, 2% SDS, 50 mM DTT, pH 8.0 and incubated 5 min at 99°C. Samples were cooled in liquid nitrogen and stored in -20°C until proteomic analysis. Total protein was determined by measuring tryptophan fluorescence as described in Wiśniewski and Gaugaz (2015).

### 2.3. Protein digestion and peptide fractionation

Protein lysates were processed in the 30K filtration units (Millipore, Darmstadt, Germany) using the MED-FASP protocol (Wiśniewski & Mann, 2012). Peptides were quantified as described previously (Wiśniewski, 2013).

### 2.4. LC – MS/MS analysis

Analysis of the peptide mixtures was performed in Orbitrap instrument (Thermo Fisher Scientific, Waltham, Massachusetts, USA) as described previously (Wiśniewski & Mann, 2012). Aliquots containing 5 µg of total peptides were chromatographed on a 50 cm column with 75 µm inner diameter packed C<sub>18</sub> material (Dr. Maisch GmbH, Ammerbuch-Entringen, Germany). Peptide separation was carried out at 300 nl/min for 75 min using a two-step acetonitrile gradient, 5%–40% over the first 60 min and 40%–95% for the following 15 min. The temperature of the column oven was 55°C.

The mass spectrometer operated in data-dependent mode with survey scans acquired at a resolution of 50,000 at  $m/z$  400 (transient time 256 ms). Up to the top 15 most abundant isotope patterns with charge  $\geq +2$  from the survey scan (300–1650  $m/z$ ) were selected with an isolation window of 1.6  $m/z$  and fragmented by HCD with normalized collision energies of 25. The maximum ion injection times for the survey scan and the MS/MS scans were 20 and 60 ms, respectively. The ion target value for MS1 and MS2 scan modes was set to  $3 \times 10^6$  and  $10^5$ , respectively. The dynamic exclusion was 25 s and 10 ppm.

The mass spectrometry data have been deposited to the ProteomeXchange Consortium via the PRIDE partner repository (Vizcaíno et al., 2013) with the dataset identifier: PXD006815.

### 2.5. Proteomic data analysis

The spectra were searched using MaxQuant software. All raw files were searched together in a single MaxQuant run. For the chymotryptic peptides generated from the GluC-pre-cleaved material a mixed Chymotryptic/tryptic specificity was set. A maximum of two missed cleavages was allowed. Carbamidomethylation was set as fixed modification. The “matching between the runs” option was used. The maximum false peptide and protein discovery rate was specified as 0.01. Protein abundances were calculated using the “total protein approach” (TPA) (Wiśniewski et al., 2014; Wiśniewski & Rakus, 2014). The calculations were performed in Microsoft Excel.

### 2.6. Immunofluorescence

Hippocampi were fixed in 4% PFA and embedded in paraffin. 4-µm sections were stained as described before

(Wiera et al., 2012). Primary and secondary antibodies with the used dilutions are listed in Supporting Information, Table S1. Tissue sections were examined with a FluoView 1000 confocal microscope (Olympus, Tokyo, Japan) at 20 $\times$  and 60 $\times$  magnification at 2,048  $\times$  2,048 picture resolution.

## 2.7. Sample collection for quantitative real-time PCR

RT-PCR, experiments were performed on two groups of female C57BL6 mice: young (P30,  $n = 4$ ) and middle-aged (13 month-old,  $n = 4$ ). Animals were anesthetized with isoflurane and decapitated and hippocampi were isolated and sliced using a McIlwain tissue chopper (TedPella, Redding, California, USA; slices were 300  $\mu\text{m}$  thick), as described previously (Ting, Daigle, Chen, & Feng, 2014). The slices were placed under stereoscope (Optatech, Warszawa, Poland) and CA1 hippocampal layers were dissected with a tip of a needle (0.3  $\times$  8 mm) and the region of stratum pyramidale of each slice was absorbed directly to TRI Reagent-containing (Applied Biosystems, Waltham, Massachusetts, USA) syringe. From each animal, 5–10 dissected stratum pyramidale samples were collected (Supporting Information, Figure S1).

## 2.8. RNA isolation and cDNA synthesis

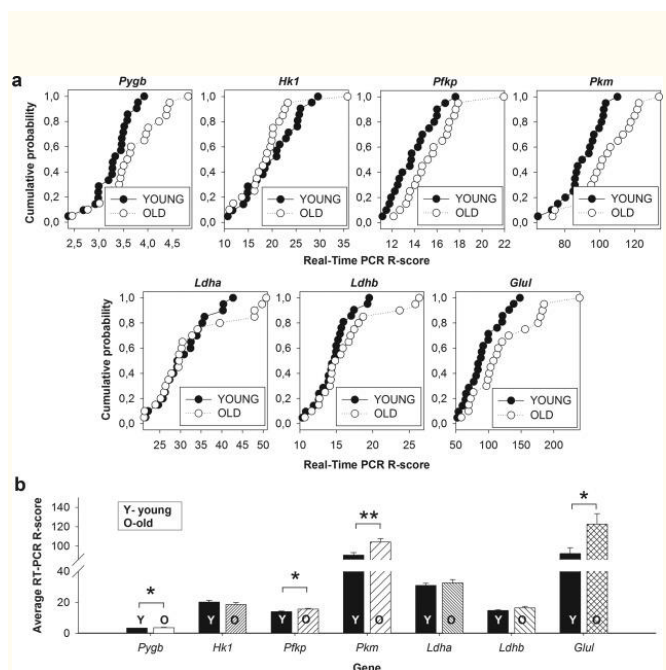
From every individual hippocampal slice, the total mRNA within CA1 stratum pyramidale region was prepared separately according to the manual (Applied Biosystems, Waltham, Massachusetts, USA). Reverse transcription was performed with total mRNA according to procedure enclosed for iScript cDNA Synthesis Kit (Bio-Rad, Hercules, California, USA). Obtained cDNA samples were used for qRT-PCR reactions. All procedures were performed with RNA-free equipment (e.g., getting rid of RNase by Ambion's RNaseZap, Thermo Fisher, Waltham, Massachusetts, USA) and DEPC-treated reagents.

## 2.9. Real-time PCR

For detection of mRNA for metabolic genes commercially available TaqMan probes (Applied Biosystems, Waltham, Massachusetts, USA) dedicated to mouse tissue were used (see Supporting Information, Table S2). The level of mRNA for glycogen synthase (*Gys1*) was used as reference (Kim et al., 2014). In

contrast to *Gys1*, our proteomic data revealed that the expression of all commonly used in qRT-PCR referential genes (Boda, Pini, Hoxha, Parolisi, & Tempia, 2009) changed during aging or they were expressed at very low levels (Supporting Information, Table S3).

Gene expression analysis was performed with iTag Universal Probes Supermix (Bio-Rad, Hercules, California, USA) and standard thermal cycling conditions using the LightCycler 480 Instrument (50 cycles of amplification). Each qRT-PCR reaction was performed in triplicate and we tested nine genes simultaneously on one plate to minimize manual handling errors. The relative gene expression level was estimated using Pfaffl algorithm and Roche LightCycler 480 Analysis Software (Basel, Switzerland). At least 20 “Young” and 20 “Old” qRT-PCR reactions for single gene were analyzed and mean relative expression level versus *Gys1* reference gene (Real Time PCR R-score) was calculated. To visualize distribution of RT-PCR R-scores between samples, results were presented in the form of cumulative histograms (Figure (Figure88a).



Upregulation of gene expression for metabolic enzymes with aging. (a) Cumulative histograms for gene expression assays for selected enzymes in brain tissue

samples collected from hippocampal CA1 region (stratum pyramidale) of young (black circles) and aged animals (white circles). Note the right-shift of the distribution of RT-PCR scores with aging in majority of investigated genes. See Section 2 for details. Abbreviations: *Pygb*, glycogen phosphorylase; *Hk1*, hexokinase 1; *Pfkip*, phosphofructokinase platelet form; *Pkm*, pyruvate kinase; *Ldha/b*, lactate dehydrogenase a/b; *Glul*, glutamine synthetase. (b) Quantification of the results shown in (a). Asterisks indicate a statistically significant difference (\* $p < .05$ , \*\* $p < .01$ )

## 2.10. Statistical analysis

All results are presented as mean  $\pm$  SEM unless otherwise stated. The statistical analysis was performed using Student's *t* test preceded by Fisher *F* test. We used non-paired Student's *t* test for comparisons between any two experimental groups. Image analysis was performed using Fiji open-source software (Schindelin et al., 2012) or Cell <sup>^</sup>F software (Olympus Soft Imaging Solutions GmbH, Tokyo, Japan). The statistical analyses were performed using SigmaPlot 11 software (Systat Software). Statistical significance of differences is indicated by asterisks: \* $p < .05$ , \*\* $p < .01$ , \*\*\* $p < .001$ .

## Results

Although steady progress has been made over recent decades, the quantitative description of basic metabolic pathways in brain is still far from being complete. Up to date, almost all studies on brain energy proteome were performed using mass spectrometry analysis of spots cut from 2D-PAGE after their densitometric measurement (for review see VanGuilder & Freeman, 2011). This makes these analyses partial and not really quantitative in terms used by biology and chemistry (for review see Gizak & Rakus, 2016). The newest, gel-free, studies of hippocampal proteome have been dedicated to investigate Alzheimer's disease-related changes and do not provide information about energy metabolism changes during aging (e.g., Neuner, Wilmott, Hoffmann, Mozhui, and Kaczorowski, 2017). In contrast, the deepest gel-free proteomic analysis of brain aging described by Walther and Mann (2011) has

been performed using adult and very old mice, respectively, 5 and 26 months-old.

Proteomically, aging significantly elevated the level of almost all glycolytic and glucose uptake proteins, however, the increase was not very high and it was in the range of 10%–20% (Supporting Information, Table S5; Figure Figure3).3). We also observed an increase in the titer of Pfk regulatory proteins (Pfkp and TIGAR) but the changes were not statistically significant (Supporting Information, Table S5). These results corroborate the findings of Freeman, VanGuilder, Bennett, and Sonntag, (2009) who have found that in rat brain, aging correlated with enhanced expression of Pfk. However, in contrast to these studies, we did not observe a chaotic dysregulation of glycolysis but a well-orchestrated increase in the level of practically all glycolytic proteins. In contrast to these proteins, among proteins associated directly with lactate metabolism and transport only the concentration of lactate dehydrogenase B was significantly modified by aging.

## Discussion

The results presented here revealed that aging correlates with entire reorganization of energy metabolism machinery, both in astrocytes and in neurons.

Glycogen degradation in brain (precisely: in astrocytes) is strictly associated with the fate of glucose described by the hypothesis called astrocytes-to-neurons lactate shuttle (ANLS), according to which astrocytic glycogen-derived lactate supports neuronal metabolism and plasticity.

Up to date, there is no convincing hypothesis of how this mechanism works. The “energetic” explanation is that the lactate being a substrate for neuronal oxidative phosphorylation may directly, via increase in ATP synthesis (for review see Obel et al., 2012), and/or indirectly, via postsynaptic changes in NADH, potentiate NMDA signaling (Yang et al., 2014). In contrast, it cannot be excluded that lactate plays a role of an autocrine signaling molecule (Morland et al., 2015). Our study support the “energetic” hypothesis, but only in young mice. In these animals, we observed distribution of crucial enzymes/proteins of energy

metabolism among astrocytes and neurons that was in agreement with the ANLS hypothesis.

However, we found that the molar ratio of Pyg to Gys (a glycogen degradation to glycogen synthesis enzyme) in hippocampus is very high and similar as in white skeletal muscle fibers (Rakus, Gizak, & Wiśniewski, 2016), which are suited for the rapid glycogen degradation. This suggests that episodes of glycogen degradation in astrocytes are rapid and thus, the short-time local increase in lactate may be sufficient to stimulate neuronal energy production in OXPHOS. By analogy to white skeletal muscle fibers, it might be hypothesized that the ANLS is highly active and significantly participates in neuronal metabolism predominantly during a high cell activity, e.g. during memory formation, when glycogen stores in astrocytes are mobilized to support neuronal OXPHOS (“LTP-ANLS”).

Furthermore, we found that concentration of glycogen metabolism enzymes significantly increased during aging. We also observed aging-associated relocation of Pygb, a regulator of glycogen degradation, and Pgm1, the enzyme directing glucose to glycogen synthesis, to neurons. Previously, we have demonstrated that in contrast to young rats, the inhibition of glycogen degradation in old animals improves neuronal plasticity and reverts aging-associated changes in LTP formation (Drulis-Fajdasz, 2015). This have led us to made an assumption that the increased level/activity of Pygb in neurons of hippocampi is the main cause of aging-associated decline in memory formation.

This work is partly presented at 9th International Conference and Expo on Proteomics and Molecular Medicine  
November 13-15, 2017 Paris, France